Hindawi
Advances in Civil Engineering
Volume 2020, Article ID 8897441, 11 pages
https://doi.org/10.1155/2020/8897441

Research Article

Frequency Spectrum and Wavelet Packet Analyses of Blasting Vibration Signals for Different Charge Structures in Blasting Peripheral Holes

Ke Man,[1] Xiaoli Liu ,[2] and Zhifei Song [1]

[1]*College of Civil Engineering, North China University of Technology, Beijing 100144, China*
[2]*State Key Laboratory of Hydroscience and Hydraulic Engineering, Tsinghua University, Beijing 100084, China*

Correspondence should be addressed to Xiaoli Liu; xiaoli.liu@tsinghua.edu.cn

Received 3 June 2020; Revised 14 September 2020; Accepted 24 September 2020; Published 12 October 2020

Academic Editor: Fengqiang Gong

Based on the blasting principle of the cutting seam cartridge, smooth blasting with the charge structures of the usual cartridge and cutting seam cartridge has been designed and implemented, respectively, for different peripheral holes in the same face. Meanwhile, the blasting vibration has been monitored. Through the analysis of the frequency spectrum of blasting vibration signals, it is found that the maximum blasting vibration velocity of the cutting seam cartridge charge is lower than that of the usual cartridge charge, from 0.21 m/s to 0.12 m/s. Moreover, the blasting energy distribution is more balanced. Especially in the low-frequency part, the blasting energy is less, and there is a transferring trend to the high-frequency part, which shows that the cutting seam cartridge charge has a better optimization effect. Furthermore, using wavelet packet analysis, the cutting seam cartridge charge could effectively reduce the energy concentration in the low-frequency part. The energy distribution is much more dispersed, and the disturbance to the structure could be less, which is conducive to the stability of the structure. According to the blasting effect, the overbreak and underexcavation quantity at the cutting seam cartridge charge is better than that at the usual cartridge charge.

1. Introduction

The directional fracture blasting technology with the cutting seam cartridge charge was originally put forward by Fourney et al. [1]. The compressive stress concentration and shear stress difference are caused along the cutting direction, which leads to the fracture surface formation under the action of blasting. As the directional fracture blasting of the cutting seam cartridge has a significant role, it is applied to underground engineering. The directional fracture blasting technology with the cutting seam cartridge charge is mainly based on the principle of shaped charge blasting. The blasting energy propagates in the way of shock waves or stress waves and explosion gas. The stress waves cause tension damage or break, and then the gas expands the crack. At the same time, it plays a good role in protecting the surrounding wall. It means that the directional fracture blasting technology with the cutting seam cartridge charge has the function of blasting energy guidance in the slit direction and the wall protection in the nonslit direction. As it is known, the purpose of the smooth blasting technique is to form a smooth final contour, and presplit blasting is to protect the remaining wall or surrounding rock mass. However, the impact of directional fracture blasting technology on the surrounding rock could also be reduced, providing a new technical access for the smooth blasting method [2, 3]. Meng et al. found that shaped charge blasting leads to the directional propagation of fractures. The field monitoring results showed that shaped charge blasting is able to realize the directional propagation of blasting-induced fractures and release mining pressure [4].

The basic principle of cutting seam cartridge blasting is shown in Figure 1. The left side is the cutting seam pipe and its longitudinal section along the diameter direction, and the right side is the detailed description of the cutting seam pipe's cross section, in which A is the longitudinal side view

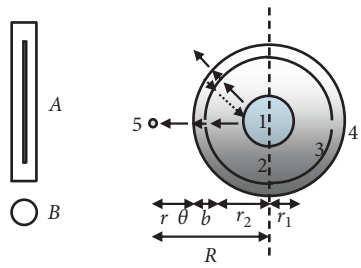

Figure 1: Schematic of the cutting seam cartridge blasting principle.

of the cutting seam pipe with a certain width, and B is the cross section of the cutting seam pipe, while 1 is the loading part, 2 is the air medium, 3 is the cutting seam pipe, 4 is the hole wall, and 5 is the rock particle with a distance R away from the center of the explosive bag.

When the cutting seam cartridge explodes, the detonation products directly impact the cutting seam pipe at the noncutting position. Because the density of the inner rock wall is greater than that of the detonation product and the compressibility of the rock wall is generally less than that of the detonation product, the detonation product reflects from the rock wall surface, and then the reflected shock wave generates. After the transmission wave is attenuated, the energy acting on the hole wall is reduced efficiently, and the possibility of radial cracks in the noncutting position is decreased significantly.

However, at the cutting direction, the detonation products directly impact the air medium. The shock wave is generated to form a concentrated, high-speed, and high-pressure jet, which is oriented on the hole wall at the cutting direction. When the strength of the stress wave is greater than the critical strength of rock mass, the fracture will occur on the blasting hole wall, and the initial fracture could be formed in advance. The detonation gas is also concentrated at the cutting direction, while the destructive and blasting effect along the cutting direction could be well strengthened.

Blasting vibration is generated at the same time, connecting with the rock dynamic strength. Zhu et al. found that the dynamic strength of deep rocks increases with increasing depth or the ratio of horizontal-to-vertical initial stresses [5, 6]. Through the analysis of blasting vibration signals, the rock-breaking mechanism and blasting effect of different blasting methods can be mastered more profoundly. Gou et al. pointed out that the average frequency and its modified frequency equation perform well in the rock mass. The soil overburden has a low impact on the ground motion, while the influence of charge weight per delay on the ground wave frequency has diminished [7, 8]. Ataei et al. found that as the blasting vibration signal is a nonstationary signal, which has the characteristics of short duration and fast mutation, its analysis mainly depends on the signal analysis mathematical methods and the development of corresponding analysis instruments [9–12].

Fourier transform is a powerful tool for vibration signal analysis [13–16]. Fourier transform is always the most widely used and effective analysis method. It is the basis and the classic technology in signal processing. It can transform the time series data to the spectrum in the frequency domain. Fourier transform is a tool of time domain to frequency domain conversion. Its essence is to decompose the signal waveform into the superposition of various sine waves with different frequencies. Its standard basis is composed of sine wave and its higher harmonics.

Hilbert–Huang transform is a breakthrough in the linear and steady-state spectral analysis based on Fourier transform. It is mainly composed of the empirical mode decomposition method and transformation [17]. According to the time difference characteristics between the adjacent peaks of the time scale signal itself, the signal could be decomposed using the Hilbert–Huang transform, which has the adaptive ability [18].

Ling et al. found that, with the increase of the blast center distance, the main frequency and amplitude of blasting waves show the decreasing trend. Besides, the frequency superposition phenomenon aggravates in the far field. It can be seen that the wavelet transform used here adopts the window size to be fixed, but its shape can be changed. It means that the time window and frequency window can be varied, while the contradiction between time resolution and frequency resolution could be solved well. Meanwhile, it has a good localization property both in time domain and frequency domain [19–21]. Wavelet transform, as an adaptive signal feature method, has been widely used in signal processing, especially in the blasting vibration, which is characterized by short duration and sudden change [22].

The concept of wavelet packet is put forward on the basis of the wavelet transform, and it is deduced mathematically. The high-frequency part which is not decomposed by the wavelet method is also conducted, and it is divided into high-frequency part and low-frequency part separately with several layers. It can adaptively select the corresponding frequency band to match the signal spectrum according to the signal characteristics, while the time-frequency resolution could be improved. Therefore, it is more precise than the wavelet analysis [23–25]. Prediction of vibration is very important in mining operations as well as civil engineering projects. Meanwhile, for the blasting vibration signal characteristics, the wavelet packet analysis of a single blasting vibration signal has been carried out, and the energy distribution is illuminated [26]. Furthermore, the blasting vibration energy in different frequency ranges of the blasting vibration signal is studied [27, 28]. In addition, other scholars have carried out the blasting vibration signal analysis of different structural forms, such as the frozen shaft [29].

For tunnel engineering, based on the principle of directional blasting fracture technology, at the peripheral hole's different positions of the same face to be excavated, two charge structures, i.e., usual cartridge charge and cutting seam cartridge charge separately, are used to compare and analyze the vibration signals and blasting effects. In particular, the wavelet packet analysis method is accepted to study the energy distribution and to explore the influence of cartridge charge way.

2. Charge Structure Design of the Peripheral Hole

In the light of actual engineering geology, the cutting seam cartridge charge and usual cartridge charge technology were designed and carried out at the same free face in the peripheral hole with the left and right positions separately. The peripheral hole of the left side uses the usual cartridge charge structure, while that of the right side adopts the cutting seam cartridge charge structure. The excavation section area is 12.15 m^2.

The peripheral hole spacing both in the left side and the right side was 300 mm. The designed footage of each blasting cycle is 2 m, and in each peripheral hole, the explosive is divided into three intervals with the same interval 550 mm. Among them, half of a cartridge was charged at the bottom of the blasting hole, and the other two quarters of the cartridge were charged at each section. As mentioned above, the peripheral hole in the right side was charged using the cutting seam cartridge structure with the above charging pattern. At the meantime, the peripheral hole in the left side was charged using the ordinary cartridge with the same charging pattern. The ordinary cartridge means that the cartridge is charged alone, and it is just a common cartridge charging way. Meanwhile, straight parallel cutting is considered and designed here.

With the directional fracture technology of the cutting seam cartridge charge structure, the section view and the longitudinal view of the blasting hole layout are designed here, as shown in Figure 2.

9 detonators with different explosion initiationtimes were designed, corresponding to the blasting sequence. It means that blasting starts from cutting holes firstly, then the auxiliary holes, to the peripheral holes, and in the end to the bottom corner holes. Usually, for the cutting holes, the blockage length is 600 mm, while for the auxiliary holes, the peripheral holes, and the other holes, it is 300 mm.

All the blasting parameters, including the number and quantity of explosives and detonator segments in each hole, are shown in Table 1, and the total explosive weight is 60.9 kg with the specific charge 2.51 kg/m^3.

3. Frequency Spectrum Analysis of the Blasting Vibration Signal

The blasting vibration signals generated by the conventional charge form and the cutting seam charge form of peripheral holes are shown in Figure 3 separately.

From the above blasting vibration signal waveform of different charge structures, it can be seen that the maximum blasting vibration velocity of the usual charge structure reaches 0.21 m/s, which is far greater than 0.12 m/s of the cutting seam charge structure. Moreover, the blasting signal of the ordinary charge is more complex, and the peak and valley changes more frequently and violently, which is not conducive to the stability of engineering facilities.

It must be noticed that the vibration waveforms given above are produced by all of the blast holes, and they should compare the frequency spectra of the vibration waves generated by the peripheral holes in the left side and the peripheral holes in the right side, while as the property of the blasting monitoring method, the vibration waveforms are produced by all of the blasting holes, and it is convenient to show the whole vibration waveform. However, it is important to focus on the specific waveforms which are just originated from peripheral holes in the two sides. Neither the monitoring method nor frequency spectra is very suitable for the testing purpose as the blasting vibration signals have not been separated well. It should be improved in the following research.

The frequency spectrum of the blasting vibration signal with the conventional charge form and cutting seam charge form of the peripheral hole is shown in Figure 4.

From the above blasting vibration signal spectrum, it can be seen that the blasting PSD (power spectrum density) accounts for a large proportion in the low-frequency segment when the usual charge is adopted, while the blasting power spectrum density accounts for a small proportion in the low-frequency segment when the cutting seam charge is considered, with a transfer to the high-frequency segment. The above signal phenomenon and its physical revelation show that the cutting seam charge has an obvious optimization effect.

4. Wavelet Packet Analysis of the Blasting Vibration Signal

When the blasting vibration signal is analyzed by the wavelet packet, the number of decomposition layers is determined by the specific signal and the working frequency band of the blasting vibration analyzer. Blasting vibration recorder 3850 developed by Chengdu Zhongke Dynamic Instrument Co., Ltd., is used for the blasting vibration test, while the minimum working frequency is 1 Hz. Since the main vibration frequency of the blasting vibration signal is generally below 200 Hz, based on the sampling theorem, the Nyquist frequency is 1000 Hz if the sampling frequency of the signal is set to 2000 Hz. According to the wavelet packet decomposition algorithm, the analysis signal can be decomposed to the fourth layer, and the corresponding minimum frequency band is 0~7.8125 Hz.

According to the theory of wavelet packet decomposition, the blasting vibration signal waveforms of different charging modes at the same measuring point are decomposed into the fourth layer by wavelet packet decomposition, and then the energy distribution at different layers could be obtained, as is shown in Figures 5 and 6, corresponding to the usual charge and cutting seam charge separately.

From the detailed decomposition of the fourth layer using the wavelet packet method, it can be seen that the energy of the blasting vibration in the range of 0–500 Hz accounts for 91.65% and 53.59% of the total energy, respectively, corresponding to the usual charge and cutting seam charge. It shows that although the energy of the blasting vibration is widely distributed in the frequency domain, most of the energy is concentrated in the range of 0~500 Hz. The energy of the usual charge is mainly concentrated in the range of 0~250 Hz, in which the energy of

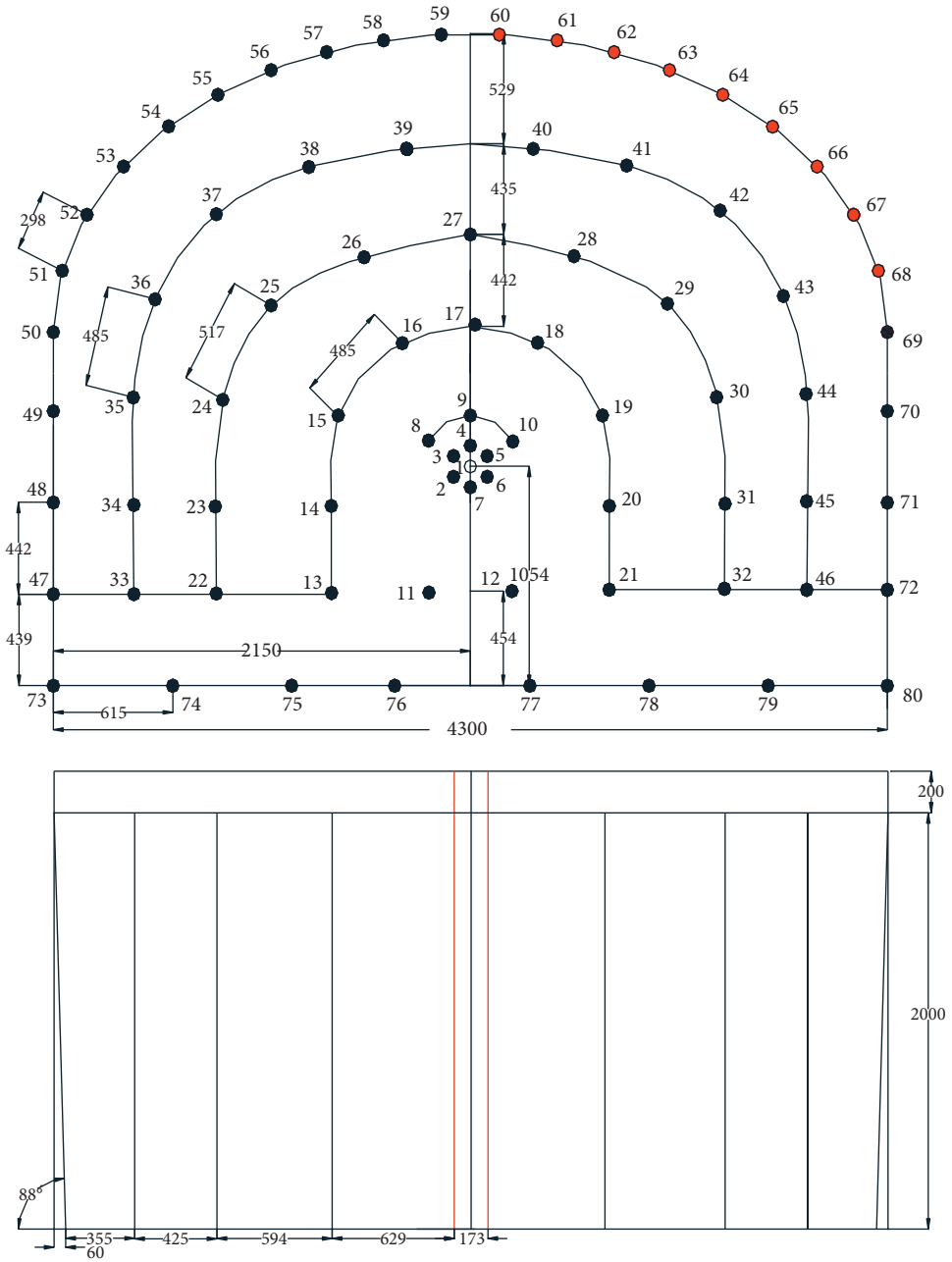

Figure 2: Section view and longitudinal view of the blasting hole of the cutting seam cartridge technology.

Table 1: Blasting parameters for the designed scheme.

Hole name	Hole no.	Sum of holes	Charge quantity		Detonator order
			Roll/each hole	Total weight (kg)	
Empty hole	1	1	0	0.0	
Cutting hole	2–7	6	5	9.0	1
Auxiliary hole	8–10	3	5	4.5	3
Auxiliary hole	11-12	2	5	3.0	5
Auxiliary hole	13–21	9	3.5	9.45	7
Auxiliary hole	22–32	11	2.5	8.25	9
Auxiliary hole	33–46	14	2.5	10.5	11
Peripheral hole	47–72	26	1.5	9.0	15
Bottom hole	74–79	6	3	5.4	17
Bottom corner hole	73,80	2	3	1.8	19
Total		80		60.9	

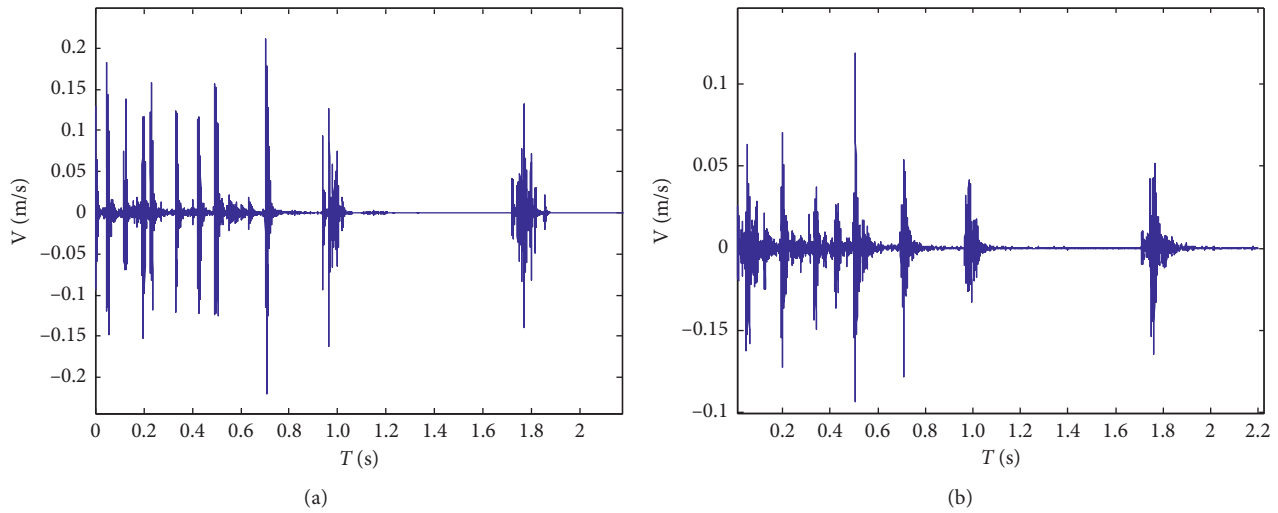

Figure 3: Typical blasting vibration waveform of the (a) usual charge and (b) cutting seam charge.

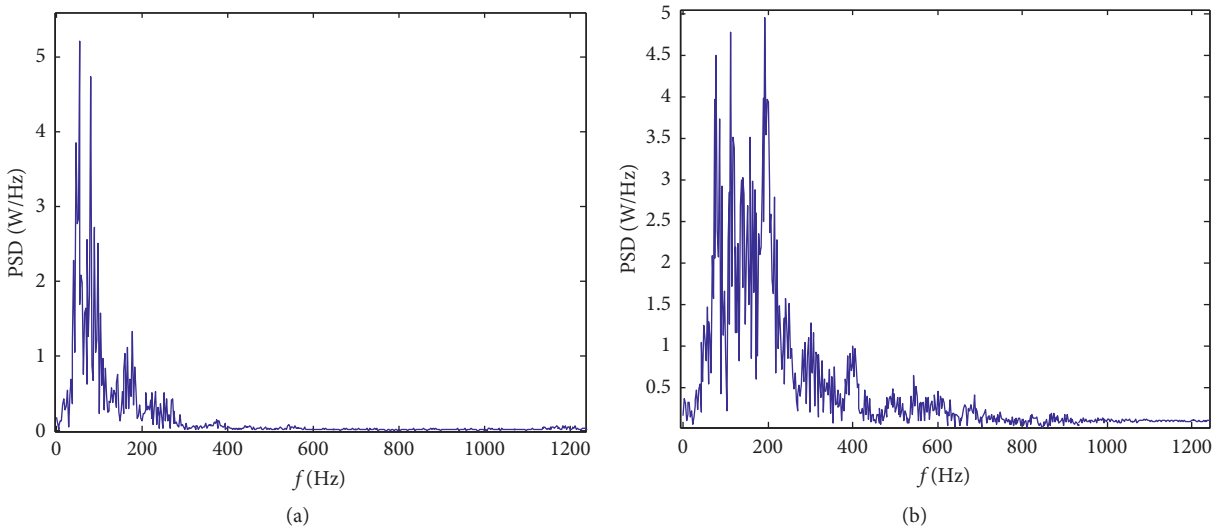

Figure 4: Power spectrum density wave of the (a) usual charge and (b) cutting seam charge.

0~250 Hz accounts for 58.11%, and the energy of 250~500 Hz accounts for 33.54%. However, the energy of the cutting seam charge is also mainly concentrated in the range of 0~500 Hz, in which the energy of 0~250 Hz accounts for 10.51%, and the energy of 250~500 Hz accounts for 43.08%.

Compared with the cutting seam charge, the energy distribution of the usual charge is more concentrated on the main vibration band. This is mainly because the blasting energy which adopted the cutting seam charge will be released rapidly along the slit direction with weak restriction. However, the single-stage explosion of the MS19 detonator reduces the mutual interference of the blasting wave, resulting in the energy more concentrated in the low-frequency band.

The energy release duration of the blasting vibration is generally short, and it has certain transient vibration characteristics. After the stress wave is transformed into the blasting vibration wave, the high-frequency component is rich and lasts for a short time when it is close to the blasting source. With the blasting vibration propagation, the high-frequency component is gradually absorbed, the vibration amplitude attenuates, the high-frequency component is smaller, and the main vibration frequency is transferred to the low-frequency segment. The vibration energy in the far region is concentrated in one or several important bands, rather than evenly distributed in each frequency band. However, by the cutting seam charge in the peripheral hole, the energy concentration in the low-frequency segment can be effectively reduced. And the energy could be more dispersed, the frequency spectrum could also be wider, and the disturbance to the structure could be much less, which is conducive to the stability of the structure. Table 2 shows the energy distribution percentage of blasting vibration signals with different charging patterns in the range of 500 Hz. It should be noticed that the testing data in Table 2, i.e., variant frequency bands and the energy distribution percentage of

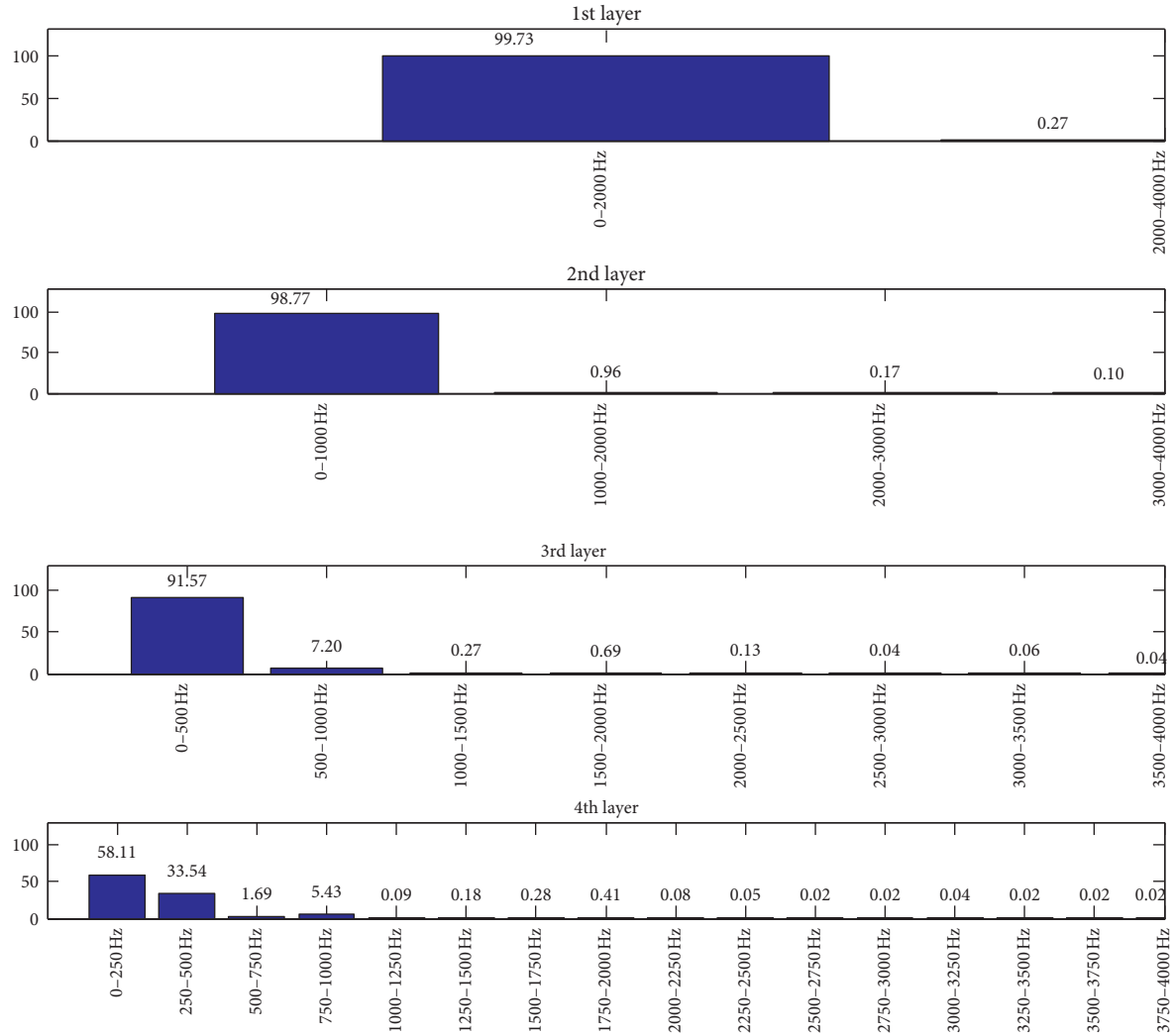

Figure 5: Energy distribution of the usual charge by wavelet packet decomposition.

blasting vibration signals for the usual charge and cutting seam charge, strictly correspond to blasting parameters designed in Table 1. Meanwhile, the data also conform to the blasting effect of the peripheral hole of the left side and that of the right side separately.

In order to refine the frequency range, energy changes within 250 Hz will be described here, as is shown in Figure 7.

The main frequency band of the blasting vibration signal is relatively wide, and the main frequency band can be divided into multiple subfrequency bands. Here, taking 8 frequency bands as an example (it means that each frequency band width is 31.25 Hz), the energy proportion within 250 Hz of the two charge forms is shown in Table 3. And it should be noticed that the original data used here are the same as those in Table 2. The other frequency spectra are not concerned as the advance frequency is within 250 Hz, which has various influences to the surrounding environment. Therefore, the frequency bands within 250 Hz are considered here.

It can be seen that the cutting seam charge plays an obvious role of frequency shift, which means that it can transfer the vibration energy from the low frequency which is unfavorable to the surrounding structures to the high frequency and weaken the phenomenon of low-frequency energy concentration.

The distance between the measuring points of the two kinds of charge forms and the explosion source is the same, but the maximum energy value of the usual charge far exceeds that of the cutting seam charge. It shows that the vibration effect could be obviously reduced by the cutting seam charge.

It should be noted that, with the increase of the maximum explosive, the main frequency of vibration tends to be within the low-frequency range. As the natural frequency of the engineering structure is generally low, it is obviously not conducive to the structure safety. Therefore, the blasting holes should be designed optimally to reduce the impact of the maximum explosive.

5. Discussion

After the blasting cycle, the footage of blasting has reached 1.7 m in the left and 1.95 m in the right, corresponding to the usual charge and cutting seam charge separately. Obviously, the

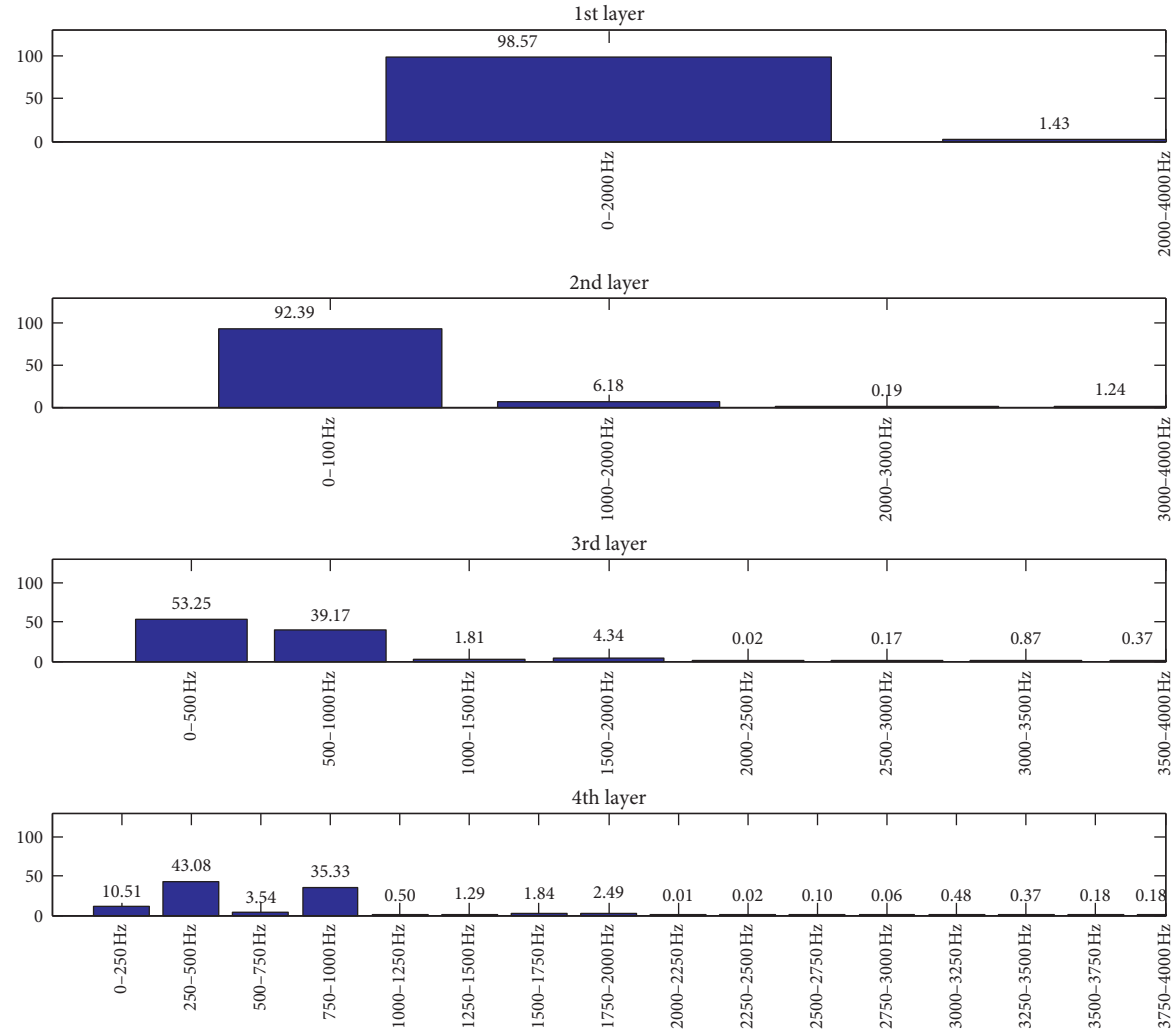

Figure 6: Energy distribution of the cutting seam charge by wavelet packet decomposition.

utilization ratio of the blasting hole in the right side is higher than that in the left side. The half-hole rate of the right side is more than 90%, and the blasting effect is smooth and even.

Image processing is carried out on the profile of the tunnel after blasting [30-36], and the ratio of overexcavation or underexcavation is calculated by the proportional image. It is found that the overexcavation quantity of the right side using the cutting seam charge is small than that of the left side. All these phenomena illuminate that using the cutting seam charge could achieve a better blasting effect.

Through the above analysis and description, the charge structure is the main reason for the difference. According to the blasting principle of the cutting seam charge, the directional fracture could be easily achieved compared to the usual charge. The rock around the surrounding hole is destroyed strictly along the cutting direction under blasting. As mentioned above, the cutting seam charge plays an important role in orientation, guidance, energy accumulation, blasting hole wall protection, and so on. The charge structure and its corresponding frequency spectrum have a much closer relationship, which reflects the blasting energy distribution delicately.

With the explosive being detonated, the blasting gas is triggered subsequently along the crack caused by the shock wave. The energy accumulates at the crack tip, and the stress concentration is more obvious, which leads to a greater dynamic stress intensity factor. When the dynamic stress intensity factor exceeds the dynamic fracture toughness of the rock, the new crack could easily extend and expand along the direction of the initial crack. All of these are much more beneficial for the subsequent action of the explosion stress wave.

Through the blasting frequency spectrum and the maximum blasting vibration velocity, the blasting effect of different charge structures is studied. It can be seen that the maximum blasting vibration velocity of the usual charge structure reaches 0.21 m/s, which is far greater than 0.12 m/s of the cutting seam charge structure. Indeed, the peak particle velocity could be achieved based on the blasting holes and the corresponding detonator. As it is mentioned above, the peak particle velocity of 0.12 m/s occurs in the sixth delay, while the following velocity is under 0.12 m/s, corresponding to the peripheral hole of the cutting seam cartridge charge. Therefore, the particle velocity could be

Table 2: Energy distribution percentage of blasting vibration signals with different charges (%).

Frequency band (Hz)	Charge of the peripheral hole	
	Usual charge	Cutting seam charge
0 ~ 7.8125	2.229991269	1.787380786
7.8125 ~ 15.625	1.039173505	1.166917023
15.625 ~ 23.4375	3.769197911	0.295469186
23.4375 ~ 31.25	1.731948796	0.863437309
31.25 ~ 39.0625	3.810539675	0.331075298
39.0625 ~ 46.875	2.889728257	0.140676688
46.875 ~ 54.6875	3.899942775	0.725965092
54.6875 ~ 62.500	2.526712103	0.36629761
62.500 ~ 70.3125	0.96876886	0.639425781
70.3125 ~ 78.125	0.655996568	0.096318144
78.125 ~ 85.9375	1.200286895	0.20576525
85.9375 ~ 93.75	0.551350271	0.151802148
93.75 ~ 101.5625	5.299342072	0.617296493
101.5625 ~ 109.375	3.166754601	0.159958934
109.375 ~ 117.1875	1.15016411	0.158657431
117.1875 ~ 125	1.491769733	0.114527373
125 ~ 132.8125	1.184100843	0.19667787
132.8125 ~ 140.625	0.581154786	0.227530343
140.625 ~ 148.4375	0.381662	0.364889045
148.4375 ~ 156.25	0.617057835	0.135266024
156.25 ~ 164.0625	2.140549217	0.210894837
164.0625 ~ 171.875	0.750862991	0.207379654
171.875 ~ 179.6875	0.696653323	1.140918129
179.6875 ~ 187.5	0.697106629	0.097205295
187.5 ~ 195.3125	2.952418532	1.961319675
195.1875 ~ 203.125	1.294974842	0.330344305
203.125 ~ 210.9375	2.00305259	0.234988512
210.9375 ~ 218.75	1.478116589	0.187356376
218.75 ~ 226.5625	1.239580217	0.611954966
226.5625 ~ 234.375	0.770995618	1.247538037
234.375 ~ 242.1875	2.087185512	0.278642608
242.1875 ~ 250	0.917105416	0.162207238
250 ~ 257.8125	0.430405954	0.820937054
257.8125 ~ 265.625	0.166238642	0.166558523
265.625 ~ 273.4375	0.152336083	0.310912838
273.4375 ~ 281.25	0.161985449	0.23733022
281.25 ~ 289.0625	0.13309732	0.431862593
289.0625 ~ 296.875	0.141422741	0.245409739
296.875 ~ 304.6875	0.126769439	1.18991625
304.6875 ~ 312.5	0.1091704	0.166339565
312.5 ~ 320.3125	0.19894952	0.375063156
320.3125 ~ 328.125	0.275914094	0.28557955
328.125 ~ 335.9375	0.207938627	0.278342079
335.9375 ~ 351.5625	0.134050918	1.168340532
351.5625 ~ 359.375	0.368801353	1.333380002
359.375 ~ 367.1875	0.19657867	0.239051763
367.1875 ~ 375	0.335578707	0.254780878
375 ~ 382.8125	0.292799121	0.270129656
382.8125 ~ 390.625	1.364984144	1.417864314
390.625 ~ 398.4375	0.440328038	0.213662935
398.4375 ~ 406.25	0.677690601	0.291063252
406.25 ~ 414.0625	0.557850063	0.275318342
414.0625 ~ 421.875	0.672880217	0.329961157
421.875 ~ 429.6875	0.528820833	0.236063615
429.6875 ~ 437.5	0.680489098	0.31556361
437.5 ~ 445.3125	0.722819807	0.234589634
445.3125 ~ 453.125	0.375598477	0.819661957
453.125 ~ 460.9375	0.363141557	0.353280394
460.9375 ~ 468.75	0.615660307	0.212132555

Table 2: Continued.

Frequency band (Hz)	Charge of the peripheral hole	
	Usual charge	Cutting seam charge
468.75 ~ 476.5625	0.450106325	0.187167038
476.5625 ~ 484.375	0.429959551	0.332138932
484.375 ~ 492.1875	0.371237143	0.213792763
492.1875 ~ 500	0.232942681	0.244471176
500 ~ 4000	8.35	46.41

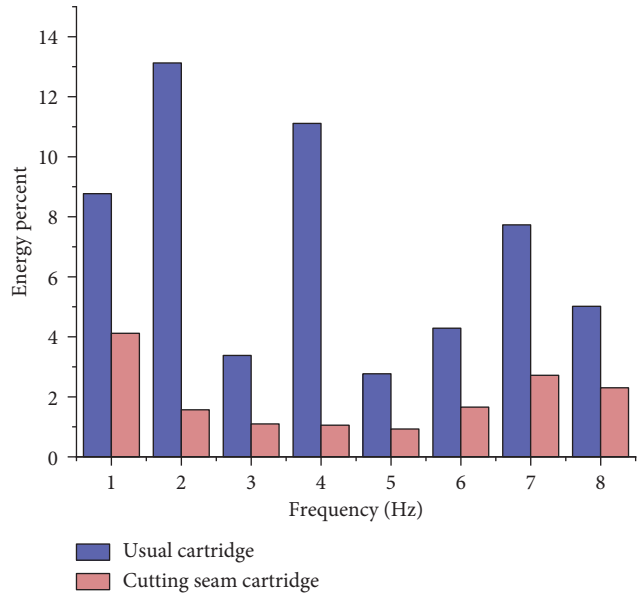

Figure 7: Energy percent distribution diagram of the usual charge and cutting seam charge during 250 Hz. 1: 0–31.25 Hz, 2: 31.25–62.5 Hz, 3: 62.5–93.75 Hz, 4: 93.75–125 Hz, 5: 125–156.25 Hz, 6: 156.25–187.5 Hz, 7: 187.5–218.75 Hz, and 8: 218.75–250 Hz.

Table 3: Energy proportion of 8 frequency bands within 250 Hz.

Usual charge	1 (0–31.25 Hz)	2 (31.25–62.5 Hz)	3 (62.5–93.75 Hz)	4 (93.75–125 Hz)
	8.77%	13.13%	3.38%	11.11%
	5 (125–156.25 Hz)	6 (156.25–187.5 Hz)	7 (187.5–218.75 Hz)	8 (218.75–250 Hz)
	2.76%	4.29%	7.73%	5.02%
Cutting seam charge	1 (0–31.25 Hz)	2 (31.25–62.5 Hz)	3 (62.5–93.75 Hz)	4 (93.75–125 Hz)
	4.11%	1.56%	1.09%	1.05%
	5 (125–156.25 Hz)	6 (156.25–187.5 Hz)	7 (187.5–218.75 Hz)	8 (218.75–250 Hz)
	0.92%	1.66%	2.71%	2.30%

reduced more for the cutting seam cartridge charge. Especially, the blasting signal of the usual charge structure is more complex, and the blasting signal's peak value changes more frequently and violently, which is not conducive to the stability of engineering facilities. Meanwhile, for the usual charge condition, the blasting power spectrum density accounts for a large proportion in the low-frequency segment. However, for the cutting seam charge condition, the blasting power spectrum density accounts for a small proportion in the low-frequency segment, with a transfer to the high-frequency segment.

Correspondingly, the overexcavation is less, and the smooth blasting effect could be improved. Therefore, the reasonable directional fracture technology using the cutting seam charge is significant.

6. Conclusion

(1) Through the analysis of the frequency spectrum of the blasting vibration signal, it is found that the maximum blasting vibration velocity of the cutting seam cartridge charge is lower than that of the usual cartridge charge.

(2) The blasting energy distribution is much more balanced using the cutting seam charge, especially in the low-frequency part. The blasting energy is less, and there is a transferring trend to the high-frequency part, which shows that the cutting seam cartridge charge has a better optimization effect.

(3) By the fourth-layer decomposition of the wavelet packet, the cutting seam cartridge charge could

effectively reduce the energy concentration in the low-frequency part. The energy distribution is much more dispersed, and the disturbance to the structure could be attenuated, which is conducive to the stability of the structure. According to the blasting effect, the overbreak and underexcavation quantity at the cutting seam cartridge charge is better than that at the usual cartridge charge.

Therefore, the wavelet packet analysis is suitable for the energy distribution and the blasting vibration in various frequency bands. The cutting seam charge structure is beneficial for the blasting effect.

Data Availability

The data that support the findings of this study are available from the corresponding author upon reasonable request.

Conflicts of Interest

The authors declare no conflicts of interest.

Acknowledgments

This work was supported by the National Natural Science Foundation of China (Grant nos. 51522903 and 51774184).

References

[1] W. L. Fourney, J. W. Dally, and D. C. Holloway, "Controlled blasting with ligamented charge holders," *International Journal of Rock Mechanics and Mining Sciences & Geomechanics Abstracts*, vol. 15, no. 3, pp. 121–129, 1978.

[2] D. J. Armaghani, E. Momeni, S. V. A. N. K. Abad, and M. Khandelwal, "Feasibility of ANFIS model for prediction of ground vibrations resulting from quarry blasting," *Environmental Earth Sciences*, vol. 74, no. 4, pp. 2845–2860, 2015.

[3] M. Hasanipanah, A. Shahnazar, H. B. Amnieh, and D. J. Armaghani, "Prediction of air-overpressure caused by mine blasting using a new hybrid PSO–SVR model," *Engineering Computations*, vol. 33, pp. 1–9, 2017.

[4] N. Meng, Y. Chen, J. Bai, X. Wang, W. Wu, and B. Wu, "simulation of directional fracturing by shaped charge blasting," *Energy Science & Engineering*, vol. 8, no. 5, pp. 1824–1839, 2020.

[5] J. B. Wang, T. Zhou, Z. Y. Liao, L. Sun, X. B. Li, and R. Chen, "Replication of internal defects and investigation of mechanical and fracture behaviour of rock using 3D printing and 3D numerical methods in combination with X-ray computerized tomography," *International Journal of Rock Mechanics and Mining Sciences*, vol. 106, pp. 198–212, 2018.

[6] J. B. Zhu, Z. Y. Liao, and C. A. Tang, "Numerical SHPB tests of rocks under combined static and dynamic loading conditions with application to dynamic behavior of rocks under in situ stresses," *Rock Mechanics and Rock Engineering*, vol. 49, no. 10, pp. 3935–3946, 2016.

[7] Y. G. Gou, X. Z. Shi, J. Zhou, and X. Qiu, "Attenuation assessment of blast-induced vibrations derived from an underground mine," *International Journal of Rock Mechanics and Mining Sciences*, vol. 127, Article ID 104220, 2020.

[8] M. Zhao, J. Zhang, and C. Yi, "Time-frequency characteristics of blasting vibration signals measured in milliseconds," *Mining Science and Technology (China)*, vol. 21, no. 3, pp. 349–352, 2011.

[9] H. B. Amnieh, A. Siamaki, and S. Soltani, "Design of blasting pattern in proportion to the peak particle velocity (PPV): artificial neural networks approach," *Safety Science*, vol. 50, pp. 1913–1916, 2012.

[10] M. Ataei and M. Kamali, "Prediction of blast-induced vibration by adaptive neuro-fuzzy inference system in Karoun 3 power plant and dam," *Journal of Vibration and Control*, vol. 19, no. 12, pp. 1906–1914, 2013.

[11] Z. P. Song, S. H. Li, J. B. Wang et al., "Determination of equivalent blasting load considering millisecond delay effect," *Geomechanics and Engineering*, vol. 15, no. 2, pp. 745–754, 2018.

[12] A. Sołtys, M. Twardosz, and J. Winzer, "Control and documentation studies of the impact of blasting on buildings in the surroundings of open pit mines," *Journal of Sustainable Mining*, vol. 16, no. 4, pp. 179–188, 2017.

[13] D. Johansson and F. Ouchterlony, "Shock wave interactions in rock blasting: the use of short delays to improve fragmentation in model scale," *Rock Mechanics and Rock Engineering*, vol. 46, no. 1, pp. 1–18, 2013.

[14] R. S. Faradonbeh, D. J. Armaghani, M. Z. A. Majid et al., "Prediction of ground vibration due to quarry blasting based on gene expression programming: a new model for peak particle velocity prediction," *International Journal of Environmental Science and Technology*, vol. 13, pp. 1453–1464, 2016.

[15] G. Ma, H. Hao, and Y. Zhou, "Assessment of structure damage to blasting induced ground motions," *Engineering Structures*, vol. 22, no. 10, pp. 1378–1389, 2000.

[16] W. Huang, Q. Xu, and W. Shen, "Application of wavelet transform in evaluation of blasting vibration damage," *Engineering Blasting*, vol. 7, no. 1, pp. 24–27, 2001.

[17] X. B. Li, Y. P. Zhang, Z. X. Liu, Y. J. Zuo, and W. H. Wang, "Wavelet analysis and Hilbert-Huang transform of blasting vibration signal," *Explosion and Shock Waves*, vol. 25, no. 6, pp. 528–535, 2005.

[18] Y. Peng, W. Lu, Y. Luo et al., "Identification of arriving time of vibration induced by geo-stress dynamic unloading during blasting excavation employing method of time-energy analysis based on wavelet transform," *Chinese Journal of Rock Mechanics and Engineering*, vol. 28, no. 1, pp. 2836–2844, 2009.

[19] T. Ling and X. Li, "Time-energy analysis based on wavelet transform for identifying real delay time in millisecond blasting," *Chinese Journal of Rock Mechanics and Engineering*, vol. 23, no. 13, pp. 2260–2270, 2004.

[20] X. L. Cao, X. W. Gao, H. T. Liu et al., "Analysis and application of blasting vibration signals based on Hilbert-Huang transform," *Acta Armamentarii*, vol. 37, no. 2, pp. 107–113, 2016.

[21] X. Li, E. Wang, Z. Li et al., "wave pattern recognition based on Hilbert-Huang transform," *Geomechanics and Engineering*, vol. 11, no. 5, pp. 607–624, 2016.

[22] D. Bie, S. Cui, and X. Li, "Wavelet packet analysis of blasting vibration signal of mountain tunnel," *Soil Dynamics and Earthquake Engineering*, vol. 117, pp. 72–80, 2019.

[23] S. Chen, W. Haixia, and A. Zhang, "Computational model and safety criterion of blasting vibration effect based on wavelet packet techniques," *Explosion and Shock Waves*, vol. 30, no. 4, pp. 377–382, 2010.

[24] X. Fu, S. Zhang, and C. Zhang, "Analysis of open-pit mining blasting vibration signals using wavelet packet method," *Engineering Blasting*, vol. 19, no. 1, pp. 24–27, 2013.
[25] T. Ling and X. Li, "The features of energy distribution for blast vibration signals in underground engineering by wavelet packet analysis," *Explosion and Shock Waves*, vol. 24, no. 1, pp. 63–68, 2004.
[26] M. Monjezi, M. Ahmadi, M. Sheikhan, A. Bahrami, and A. R. Salimi, "Predicting blast-induced ground vibration using various types of neural networks," *Soil Dynamics and Earthquake Engineering*, vol. 30, no. 11, pp. 1233–1236, 2010.
[27] L. Bahrami, L. Yuan, and Q. Xie, "Decomposition and energy distribution of blasting vibration signal based on second generation wavelet packet," *Explosion and Shock Waves*, vol. 33, no. 2, pp. 140–147, 2013.
[28] G. Zhong, L. Ao, and K. Zhao, "Influence of explosion parameters on energy distribution of blasting vibration signal based on wavelet packet energy spectrum," *Explosion and Shock Waves*, vol. 29, no. 3, pp. 300–305, 2009.
[29] R. Shan, B. Yao, and Y. Song, "Wavelet packet analysis of blast vibration signals of freezing shaft model," *Journal of China Coal Society*, vol. 41, no. 8, pp. 1923–1932, 2016.
[30] X. Liu, G. Han, E. Wang, S. Wang, and K. Nawnit, "Multiscale hierarchical analysis of rock mass and prediction of its mechanical and hydraulic properties," *Journal of Rock Mechanics and Geotechnical Engineering*, vol. 10, no. 4, pp. 694–702, 2018.
[31] Q. Du, X. Liu, E. Wang, and S. Wang, "trength reduction of coal pillar after CO_2 sequestration in abandoned coal mines," *Minerals*, vol. 7, no. 2, p. 26, 2017.
[32] G. He, E. Wang, and X. Liu, "Modified governing equation and numerical simulation of seepage flow in a single fracture with three-dimensional roughness," *Arabian Journal of Geosciences*, vol. 9, p. 81, 2016.
[33] Y. Yu, E. Wang, J. Zhong et al., "Stability analysis of abutment slopes based on long-term monitoring and numerical simulation," *Engineering Geology*, vol. 183, pp. 159–169, 2014.
[34] Q. Lv, E. Wang, X. Liu, and S. Wang, "Determining the intrinsic permeability of tight porous media based on bivelocity hydrodynetics," *Microfluidics and Nanofluidics*, vol. 165, no. 5, pp. 841–848, 2014.
[35] X. Liu, F. Wang, J. Huang, S. Wang, Z. Zhang, and K. Nawnit, "Grout diffusion in silty fine sand stratum with high groundwater level for tunnel construction," *Tunnelling and Underground Space Technology*, vol. 93, Article ID 103051, 2019.
[36] H. Sun, X. L. Liu, and J. B. Zhu, "Correlational fractal characterisation of stress and acoustic emission during coal and rock failure under multilevel dynamic loading," *International Journal of Rock Mechanics and Mining Sciences*, vol. 117, pp. 1–10, 2019.